Probabilistic Tsunami Hazard Analysis of Batukaras Village as a Tourism Village in Indonesia

Wiwin Windupranata[1], M. Wahyu Al Ghifari[2], Candida A. D. S. Nusantara[3], Marsyanisa Shafa[2], Intan Hayatiningsih[2], Iyan E. Mulia[1,4], Alqinthara Nuraghnia[2]

[1]Research Group of Hydrography, Faculty of Earth Sciences and Technology, Institut Teknologi Bandung, Bandung, 40116, Indonesia
[2]Study Program of Geodesy and Geomatics Engineering, Faculty of Earth Sciences and Technology, Institut Teknologi Bandung, Bandung, 40116, Indonesia
[3]Department of Geomatics Engineering, Faculty of Civil Planning and Geo Engineering, Institut Teknologi Sepuluh Nopember, Surabaya, 60111, Indonesia
[4]RIKEN Cluster for Pioneering Research, Prediction Science Laboratory, Japan

Correspondence to: Wiwin Windupranata (w.windupranata@itb.ac.id)

Abstract. Indonesia's location in the middle of tectonic plates makes it vulnerable to earthquakes and tsunamis, especially in the megathrust zone around Sumatra Island and the southern part of Java Island. Research shows a seismic gap in southern Java, which poses a potential threat of megathrust earthquakes and tsunamis, impacting coastal areas such as Batukaras Village in West Java, a popular tourist destination. To prepare for disasters, Probabilistic Tsunami Hazard Analysis (PTHA), which focuses on seismic factors, was carried out by modeling tsunamis on 3,348 sub-segments of 4 large megathrust segments in the south of Java Island. Stochastic earthquake modeling to simulate the occurrence of a tsunami from an earthquake with 6.5 Mw to the highest potential magnitude on. This research shows that PTHA in Batukaras Village reveals varying heights of 0.84 m, 1.63 m, 2.97 m, and 5.7 m for each earthquake return period of 250 years, 500 years, 1000 years, and 2500 years. The dominant threat arises from the West Java-Central Java megathrust segment, emphasizing the importance of preparedness, although the annual probability of tsunamis is generally low. Our study will deepen knowledgeof tsunami hazards associated with megathrust activities near Batukaras Village for mitigation planning and decision-making, and it can become a reference for similar coastal tourist areas.

1 Background

Indonesia is located in the convergent boundaries between several tectonic plates, making it prone to earthquakes and tsunamis. The meeting between these plates causes the emergence of a zone called the megathrust zone. Megathrust is a type of fault that occurs in the subduction zone of one tectonic plate forced under another plate. High seismic activity in Indonesia occurs around Sumatra and southern Java due to the megathrust zone (Koswara et al., 2021; Mulia et al., 2019; Supendi et al., 2023; Windupranata et al., 2020).

Research conducted by Supendi et al. (2023) shows a seismic gap to the south of the island of Java that has a potential source of future megathrust earthquakes. This potential earthquake could generate tsunami heights of up to 20 meters on the south coast of West Java, with an average maximum height of 4.5 meters along the south coast of Java. The annual probability of a tsunami event with a height of more than 3.0 meters that could cause significant loss of life and damage has a probability of 1-10% in the South of Java (Horspool et al., 2014). An earthquake occurred in Pangandaran Regency on 17 July 2006 with a magnitude of 7.6 Mw that generated a powerful tsunami (Fujii & Satake, 2006; Gunawan et al., 2016; Hanifa et al., 2014). This event resulted in more than 300 deaths, 301 serious injuries, 551 minor injuries, and 156 people missing (Mustafida et al., 2022). Other research shows that there is still a high tsunami potential due to the megathrust fault in southern Java, which has an earthquake return period of 500 years (Harris et al., 2019). This condition is reinforced by the fact that no major earthquakes have occurred in the past few years; only earthquakes of magnitude below Mw<8 have occurred in the past 100 years (Supendi et al., 2023). This means that megathrust earthquakes still have the potential to occur.

Meanwhile, the southern part of Java has high tourism potential to be developed. One of these tourism potentials can be seen from the many tourist villages located on the southern coast of Java, one of which is Batukaras Village, located in Pangandaran Regency, West Java (Koswara et al., 2021; Nijman, 2021; Windupranata et al., 2020). Batukaras Village is one of the villages in Indonesia that is often visited by local and foreign tourists. Every year, tourists visiting Batukaras can reach 521,000 people (before the pandemic) (Batukaras Village Profile, 2022). Batukaras Village itself is inhabited by 5,172 residents with a density of 393 people/km^2, where this population is vulnerable to tsunami disasters. Then, the coast of Batukaras Village is dominated by lodging places, restaurants, as well as plantation and agricultural land. Therefore, the preparedness of this tourist village in facing the tsunami disaster needs to be reviewed to minimize casualties and economic losses.

Tsunami hazard analysis in this tourist village can be done by modeling the tsunami using Probabilistic Tsunami Hazard Analysis (PTHA). The PTHA method is an approach that can estimate the tsunami hazard in a certain period of time in each area that is likely to be exposed to the hazards of the tsunami disaster (Grezio et al., 2017). This method can analyze tsunami hazards originating from seismic (plate tectonic activity) or non-seismic (volcanic activity, submarine landslides, and other events) factors (Grezio et al., 2017; Salmanidou et al., 2019). However, the scenario of potential tsunami hazards from these non-seismic factors is poor, as the timing and mechanism of their occurrence are difficult to estimate (Grezio et al., 2017). In addition, most tsunamis that occur in Indonesia are caused by seismic factors, i.e., vertical displacement of the seabed caused by shallow earthquakes in subduction zones (Hamzah et al., 2000).

In this study, tsunami modeling based on seismic factors will be conducted using the parameters of megathrust plate activity directly adjacent to Batukaras Village. The results of the PTHA analysis are expected to characterize the tsunami hazard at the study site, thereby facilitating mitigation planning and decision-making. In addition, Batukaras Village is currently in the process of being recognised as a tsunami ready village that refers to 12 IOC-UNESCO indicators consisting of assessment, preparedness, and response components (Mustafida et al., 2022). The results of this PTHA analysis can support the assessment

component to make this village a tsunami ready village issued by IOC-UNESCO. Furthermore, the results of the tsunami hazard analysis in this village can be used as a reference for other tourist villages, especially for areas that have similar characteristics to Batukaras Village.

2 Data and Method

2.1 Data

In this research, accurate bathymetry data will determine the quality of tsunami modeling results. Bathymetry data was obtained from BATNAS (National Bathymetry) provided by the Indonesian Geospatial Information Agency (BIG). This data was used to create the wave propagation domain of the tsunami modeling. Furthermore, earthquake generation parameter data were obtained from the National Centre for Earthquake Studies (PuSGEN) in 2017 and the United States Geological Survey (USGS). The earthquake parameter data is divided into rake, dip, slip, strike, length, and width data obtained from PuSGEN and the depth of the epicenter data obtained from USGS.

2.2 Method

PTHA was used as hazard modeling to determine the tsunami risk in Batukaras Village. This method is used to determine the tsunami hazard in an area with a geographically consistent approach to estimating long-term hazards, including uncertainties in the analysis (Grezio et al., 2017) and modeling parameters (Thio et al., 2007). In the process of tsunami analysis using the PTHA method, several stages of data processing must be carried out.

2.2.1 Tsunami Green's Function

The calculation of Green's Function aims to obtain the height of the tsunami wave from each observation point. In the calculation of Green's function, domain creation, megathrust sub-segments, and determination of observation points are carried out.

In this tsunami modelling, two types of model domains are formed, namely domain 1 and domain 2. Domain 1 is a large area covering the study area, namely Batukaras Village and the megathrust segment. The megathrust segment used in this tsunami modelling includes the megathrust segments of the Sunda Strait, West Java-Central Java, East Java and Bali (Figure 2). Domain 2 is a smaller area that only covers the study area of Batukaras Village, which is located in Pangandaran Regency.

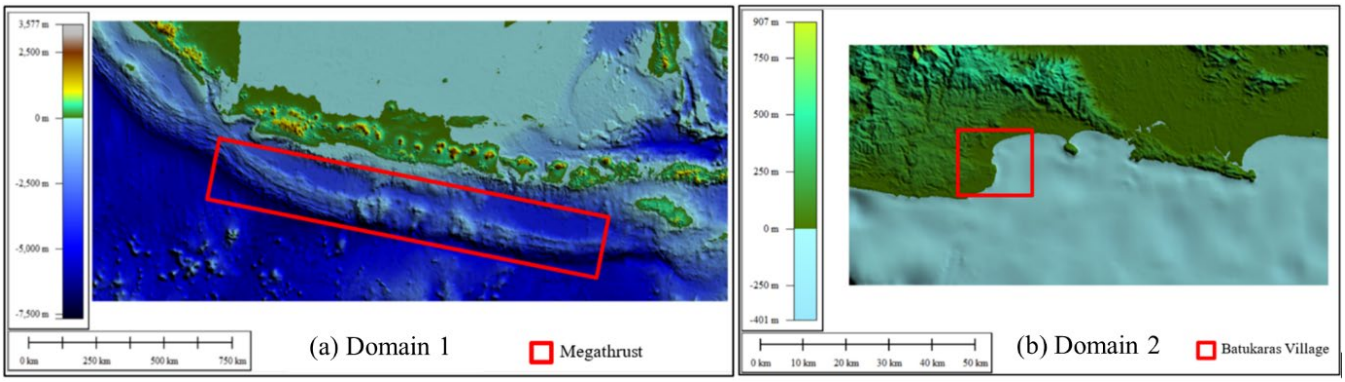

Figure 1 Modeling domain ilustration (a) Domain 1 (b) Domain 2

In this tsunami modelling, data on the four segments such as location and segment size were sourced from PuSGEN in 2017. Furthermore, the four segments were modelled as megathrust sub-segments with a grid size of 10 kilometres x 10 kilometres, resulting in 3,348 sub-segments divided into:

- Sunda Strait segment (612 sub-segments).
- West Java-Central Java segment (800 sub-segments).
- East Java segment (736 sub-segments).
- Bali segment (1200 sub-segments).

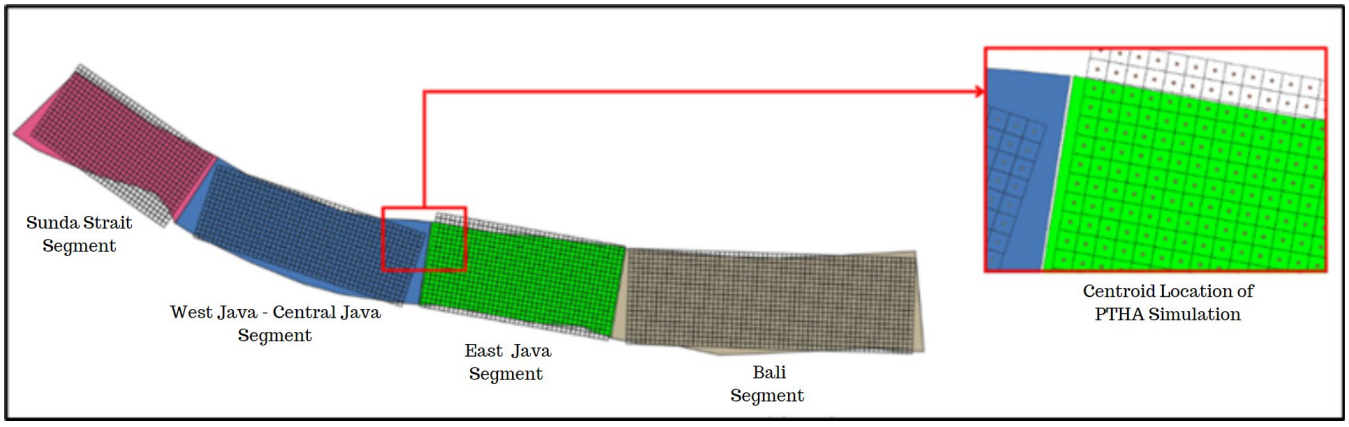

Figure 2 Megathrust sub-segment used in PTHA Modeling

In this tsunami modelling, the location of observation points was determined to evaluate the height of the tsunami generated each observation point. The locations of these observation points are spread along the coastline in Batukaras Village. In this modelling, 20 observation points were used based on bathymetry data, where the location of each point has an isobath (depth) of 1 meter.

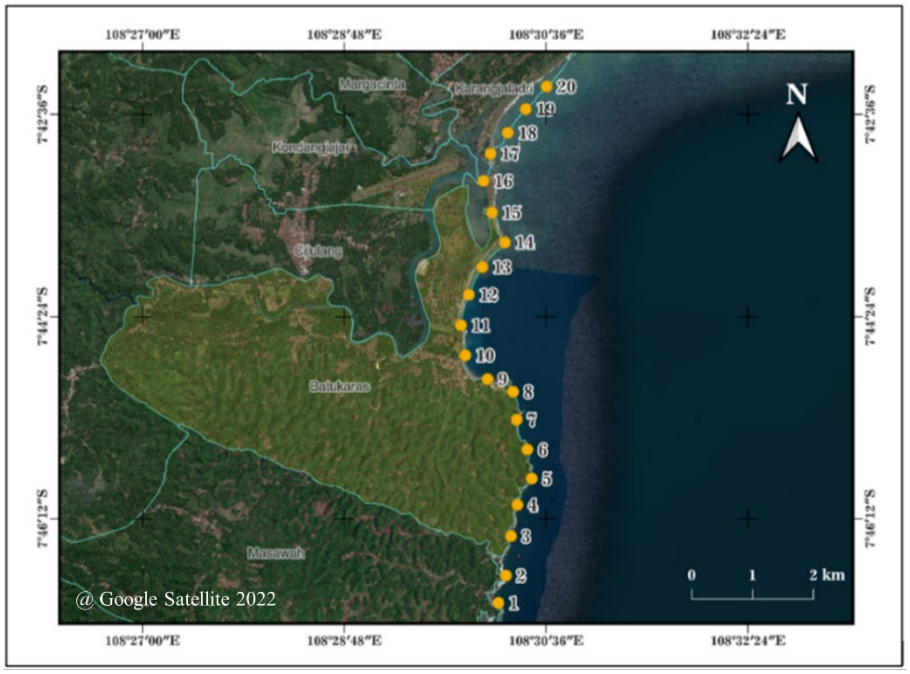

Figure 3 Observation point along Batukaras coast

We used the Cornell Multi-Grid Coupled Tsunami (COMCOT) software version 1.7 for tsunami modelling. In COMCOT, modelling is carried out by generating waves from earthquakes originating from megathrust segments based on earthquake parameter data and propagating the tsunami waves using the shallow water equation to obtain tsunami heights at each observation point. This tool only simulates tsunami waves with no influence of wind and tides.

The COMCOT software uses the Linear Shallow Water Equation (LSWE) and the Non-Linear Shallow Water Equation (NLSWE). The LSWE equation is used when tsunami waves are still in the open sea with smaller wave amplitude compared to depth. The following is the LSWE equation used (Wang, 2009).

$$\frac{\delta\eta}{\delta t}+\frac{1}{Rcos\varphi}\left\{\frac{\delta P}{\delta\psi}+\frac{\delta}{\delta\psi}(cos\varphi Q)\right\}=\frac{-\delta h}{\delta t} \quad (1)$$

$$\frac{\delta P}{\delta t}+\frac{gh}{Rcos\varphi}\frac{\delta\eta}{\delta\psi}-fQ=0 \quad (2)$$

$$\frac{\delta Q}{\delta t}+\frac{gh}{R}\frac{\delta\eta}{\delta\psi}+fP=0 \quad (3)$$

$$\frac{\delta\eta}{\delta t}+\frac{1}{Rcos\varphi}\left\{\frac{\delta P}{\delta\psi}+\frac{\delta}{\delta\varphi}(cos\varphi Q)\right\}=\frac{-\delta h}{\delta t} \quad (4)$$

$$\frac{\delta P}{\delta t} + \frac{1}{Rcos\varphi}\frac{\delta}{\delta\varphi}\left\{\frac{P^2}{H}\right\} + \frac{1}{R}\frac{\delta}{\delta\varphi}\left\{\frac{PQ}{H}\right\} + \frac{gh}{Rcos\varphi}\frac{\delta\eta}{\delta\varphi} - fQ + F_x = 0 \quad (5)$$

$$\frac{\delta P}{\delta t} + \frac{1}{Rcos\varphi}\frac{\delta}{\delta\varphi}\left\{\frac{P^2}{H}\right\} + \frac{1}{R}\frac{\delta}{\delta\varphi}\left\{\frac{PQ}{H}\right\} + \frac{gh}{Rcos\varphi}\frac{\delta\eta}{\delta\varphi} - fQ + F_x = 0 \quad (6)$$

$$\frac{\delta Q}{\delta t} + \frac{1}{Rcos\varphi}\frac{\delta}{\delta\psi}\left\{\frac{P^2}{H}\right\} + \frac{1}{R}\frac{\delta}{\delta\varphi}\left\{\frac{PQ}{H}\right\} + \frac{gh}{R}\frac{\delta\eta}{\delta\varphi} + fP + F_y = 0 \quad (7)$$

Then, when the tsunami wave travels in shallow waters, the NLSWE equation is used. This is because the wavelength becomes shorter and the wave amplitude becomes larger when passing through shallow water. This means that the shape of the seabed influences the wave amplitude. The following is the NLSWE equation used (Wang, 2009).

$$H = \eta + h \quad (8)$$

$$f = \Omega sin\varphi \quad (9)$$

$$F_x = \frac{gn^2}{H^{7/3}} P\sqrt{P^2 + Q^2} \quad (10)$$

$$F_y = \frac{gn^2}{H^{7/3}} Q\sqrt{P^2 + Q^2} \quad (11)$$

$$P = \int_{-h}^{\eta} udz = u(h + \eta) = uH \quad (12)$$

$$Q = \int_{-h}^{\eta} vdz = v(h + \eta) = uH \quad (13)$$

Where g = acceleration of gravity m/s^2; P = volume flux in-x (West-East) m/s^2; Q = volume flux in-y (South - North) m/s^2; f = Coriolis force coefficient; (φ, ψ) = latitude and longitude (°); R = radius of the earth (m); h = water depth (m); η = water surface height (m); H = total water depth (m); Ω = earth rotation rate (7.2921 x 10^{-5} rad/s); (Fx, Fy) = bottom friction at -x and -y; n = manning roughness coefficient (s/m$^{1/3}$); u = current velocity in -x (m/s); v = current velocity in -y (m/s).

2.2.2 Stochastic Earthquake Modeling

Stochastic earthquake modelling aims to simulate the slip amount on the fault plane, determining the initial seafloor displacement and the corresponding tsunamis. Mai and Beroza (2002) developed a method to characterise the complexity of earthquake slip represented by spatially random fields of anisotropic wave number spectra according to the von Karman autocorrelation function. The stochastic nature of the method is associated with uniformly distributed random phase angles

embedded in the domain. In this study random slips are initially calculated at a 1 km grid spacing and then interpolated into the sub-segment size for tsunami Green's function calculation. In this study, bilinear interpolation is performed without changing the average slip, thus maintaining the magnitude of the moment of the interpolated sample. In the formation of the stochastic earthquake model, several settings were used including:

1. The minimum magnitude value used is 6.5 Mw sourced from USGS.
2. The maximum magnitude value used is sourced from PuSGEN in 2017. The maximum magnitude value used is different for each megathrust segment. The Sunda Strait segment has a maximum magnitude of 8.8 Mw; West Java-Central Java of 8.8 Mw; East Java of 8.9 Mw; and the Bali Segment of 9 Mw.
3. The earthquake magnitude bin (interval) used in the modelling is 0.1 Mw, so the earthquake will be generated starting from the minimum magnitude to the maximum magnitude with a difference of 0.1 Mw.
4. The rupture area is randomly specified within the megathrust segment, as done in the PTHA study by Mori et al. (2017).

Figure 4 shows examples of the resulting slip distribution from various earthquake magnitudes by Mulia et al., (2020).

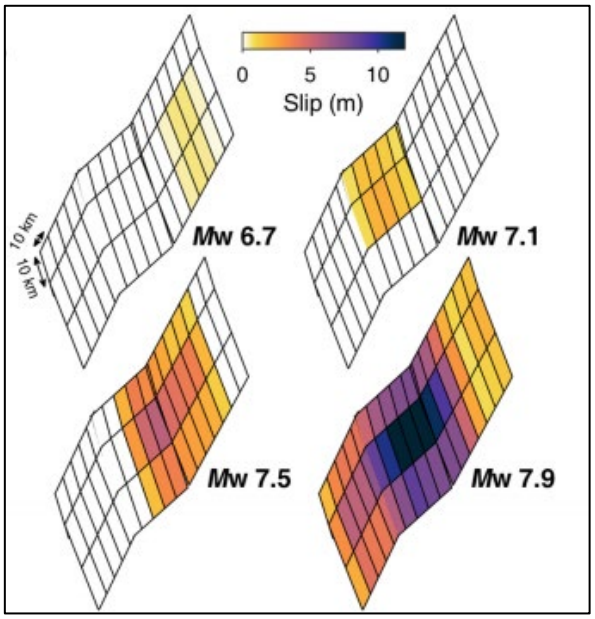

Figure 4 Stochastic earthquake generation illustration (Mulia et al., 2020)

We also conducted statistical analyses that show the level of variability in each magnitude range. This analysis uses the coefficient of variation (CV) = σ/μ, where σ is the standard deviation and μ is the mean of maximum coastal tsunami heights at all coastal points. This analysis reflects the convergence of Monte Carlo samples of tsunami heights in coastal areas associated with the sources of the identified active faults, so that the number of samples required across the earthquake magnitude range can be estimated.

We performed this calculation for each increment of magnitude bin (Mw 0.1) of the earthquake in the interval Mw 6.5 to Mw 9.0. The maximum magnitude values used were sourced from PuSGEN in 2017 such as in the Sunda Strait (Mw 8.8), West Java-Central Java (Mw 8.8), East Java (Mw 8.9), and Bali (Mw 9.0) segments. At each magnitude interval, we calculated the coefficient of variation with each increase in the number of samples from 2 to 150.

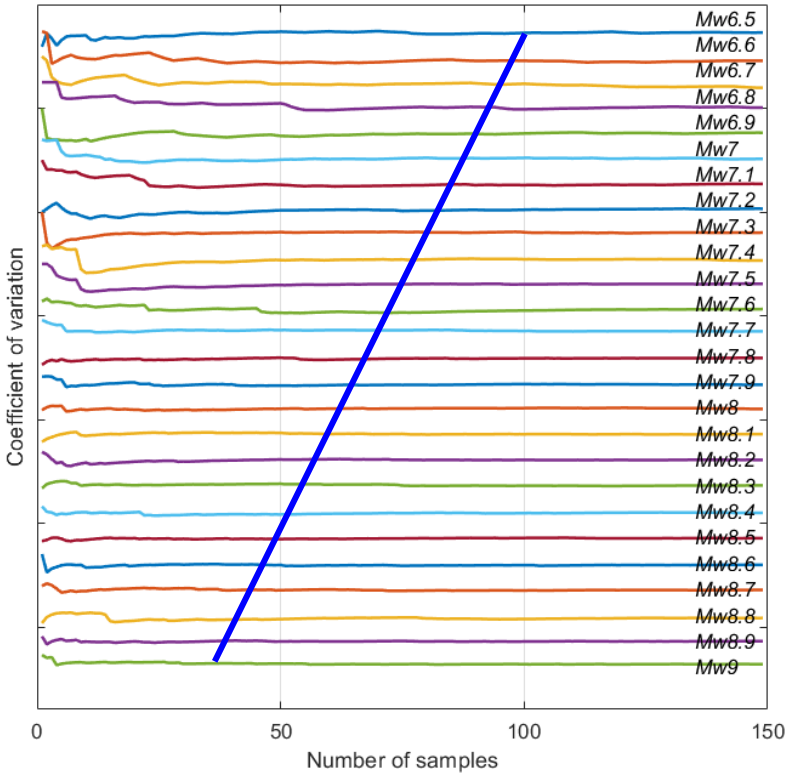

Figure 5 Coefficient of variation of maximum coastal tsunami height for each magnitude across megathrust segments. The blue line indicates the number of samples required at each magnitude bin for the PTHA

In figure 5 it can be seen that the variability value decreases as the magnitude increases due to randomisation of the rupture area from smaller earthquakes. Each magnitude shows different variability. For example, the height of a coastal tsunami caused by a Mw 6.5 earthquake is quite stable if about 100 samples are used. Therefore, in this study we assume that the minimum number of samples required is 100 for Mw 6.5. Using a visual approach, we also applied it to all magnitudes by drawing a straight line (blue coloured line). This line shows the number of earthquake scenarios required for each magnitude. Thus, the resulting number of scenarios is 7,019 scenarios. This large number of scenarios is expected to provide a good explanation of the epistemic uncertainty of the PTHA results in this study.

Table 1 Total samples at each magnitude bin

No.	Mw	Number of faults with magnitude Mw (A)	Number of samples at each magnitude bin (B)	Total samples at each magnitude bin = A×B
1.	6.5	4	100	400
2.	6.6	4	98	392
3.	6.7	4	95	380
4.	6.8	4	92	368
5.	6.9	4	90	360
6.	7.0	4	88	352
7.	7.1	4	85	340
8.	7.2	4	83	332
9.	7.3	4	80	320
10.	7.4	4	77	308
11.	7.5	4	75	300
12.	7.6	4	73	292
13.	7.7	4	71	284
14.	7.8	4	68	272
15.	7.9	4	65	260
16.	8.0	4	63	252
17.	8.1	4	61	244
18.	8.2	4	58	232
19.	8.3	4	56	224
20.	8.4	4	53	212
21.	8.5	4	51	204
22.	8.6	4	49	196
23.	8.7	4	47	188
24.	8.8	4	45	180
25.	8.9	2	43	86
26.	9.0	1	41	41
		Total scenario		7019

2.2.3 Determination of a and b Values Modelling

160 The values of a and b in PTHA are constants from the empirical formula derived by B. Gutenberg and C. F. Richter with the equation (Gutenberg & Richter., 2010).

$$logN(M) = a - bM \quad (14)$$

Where N is the earthquake frequency; M is the magnitude; a and b are constants.

This equation shows the relationship between earthquake frequency and magnitude. The values of a and b indicate the seismic activity of the megathrust segment, which is influenced by the degree of rock fragility, and these values depend on the observation period, the area of observation, and the seismicity in the area. The larger the value of a for a segment indicates that the segment has high seismic activity; the larger the value of b indicates that the degree of rock fragility in the segment is higher. In this study, the values of a and b were not calculated. Instead, they were sourced from PusGEN in 2017.

2.2.4 Probabilistic Tsunami Hazard Analysis (PTHA) Calculation

In this tsunami modelling, the modelling basis is used, which can be seen in the Table 2.

Table 2 General parameter for Tsunami modeling

Parameter	Domain	
	1	2
Simulation Time (second)	18,000	18,000
Save Time Interval (second)	60	60
Reference Domain	0	1
Grid Size (meter)	1800	600

Based on Table 2, the simulation time used for each tsunami scenario run is 6 hours. In addition, earthquake parameter data sourced from USGS and PuSGEN in 2017 were also determined. Earthquake parameters such as depth, strike, slip, and dip were obtained from the USGS slab 2.0 model, with the rake angle considered opposite to the direction of plate movement in the interseismic phase (Hayes et al., 2018). Meanwhile, the parameters of the epicentre and megathrust segmentation were obtained from the results of the PusGEN study in 2017.

Probabilistic seismic hazard assessment was introduced by (Cornell C. Allin, 1968), which was then adopted in PTHA to predict the rate of exceedance of a certain tsunami height (H) relative to the tsunami height level (h), which in discrete form can be formulated in equation 15.

$$\lambda(H \geq h) = \sum_{i=1}^{n_s} vi \sum_{j=i}^{n_m} P(H \geq h|m_j) P(M_i = m_j) \quad (15)$$

Where, n_s is the total number of i sources/faults; n_m is the number of magnitudes m considered with j intervals; m is the magnitude bin; υ is the occurrence rate of earthquakes from each common plate; and P is the probability of tsunami height.

In this study, a magnitude ranges from the smallest magnitude to the largest magnitude with a magnitude bin of 0.1 is considered. The variable υ indicates the occurrence rate of earthquakes with M equal to or greater than each fault calculated using the Gutenberg-Richter frequency magnitude distribution (Gutenberg & Richter 1944). The variable υ can be defined by the equation shown in equation 16.

$$v = 10^{a-bm}min \tag{16}$$

Next, the probability of tsunami height is calculated. The probability that the tsunami height H exceeds any tsunami height level given the magnitude m can be expressed as:

$$P(H \geq h|m) = 1 - \Phi\left\{\frac{ln(h) - ln(H)}{\beta}\right\} \tag{17}$$

With the cumulative standard-normal distribution function (Φ), the median logarithmic tsunami height of all models with a given source and magnitude represented by ln(H), and β is the standard deviation of ln(H).

Based on PTHA Manual by Thio (2012), a crucial aspect of a probabilistic hazard analysis is the incorporation of uncertainties in both the source and propagation models into the final outcome. There are two types of uncertainties: aleatory and epistemic. These uncertainties belong to frequency and degree of belief approaches to probability respectively.

Aleatory uncertainties refer to the inability to predict the outcome of a process due to its random nature. However, it may not always be clear whether an uncertainty in the outcome of a process is a true aleatory uncertainty caused by the random behavior of nature, or a result of a limited understanding of the process itself. In such cases, researchers may have differing opinions. To express the outcome of a process that involves aleatory uncertainties, distribution functions are used rather than single mean or median values. The probability of an outcome being within a certain range is then given by the area under the probability density or distribution function. We have identified three main sources of aleatory uncertainty in our analysis, which are modeling uncertainty (σ_A), uncertainty in geometry (σ_D), and uncertainty in random slip distribution (σ_S).

The parameter β in equation 17 is included to account for aleatory uncertainty related to tsunami simulations and source uncertainties. Thio (2012) and Horspool et al. (2014) use combined uncertainty with a total β value of 0.519, while Davies et al. (2018) uses the square root of the β values obtained from four historic tsunamis which results in a larger β value of 0.927. Annaka et al. (2007) and Fukutani et al. (2015) have also treated β as epistemic uncertainty using a logic-tree approach. In this approach, β ranges from 0.223 to 0.438, corresponding to κ values of 1.25 to 1.55. The β value can be estimated from the logarithmic standard deviation κ of Aida (1978) where $\beta = \ln(\kappa)$ as we will use in this research. To obtain logarithmic standard deviation κ we compared the height of historical tsunami waves in Pangandaran 2006 from (Fritz et al., 2007) with the

modelling scenario that has the closest characteristics to the historical tsunami waves. Then the κ value is calculated in accordance with Aida (1978) and the β can be obtained. Based on the 2006 Pengandaran tsunami, the value of β is 1.0999.

3 Result and Discussion

Based on the PTHA that has been carried out, several products are obtained that can be used as material for analysis to determine the level of tsunami hazard in Batukaras Village.

3.1 Tsunami Hazard Curve

The first product of the PTHA is the tsunami hazard curve. The hazard curve is a curve that describes the relationship between the tsunami intensity value and the return period of an earthquake at an observation point (Grezio et al., 2017). The tsunami hazard curve for Batukaras Village can be seen in Figure 6.

Based on the hazard curve, the level of hazard can be seen from the probability of tsunami wave heights occurring in Batukaras Village at each observation point. In this case, twenty observation points were used, spread along the coastline of Batukaras Village. In addition, the mean and median values of the tsunami height can also be seen. As can be seen from Figure 6, at an earthquake return period of 100 years, the tsunami height in Batukaras Village does not reach 1 meter, but as the earthquake return period increases, the tsunami height will increase to 10 meters at an earthquake period of 10,000 years.

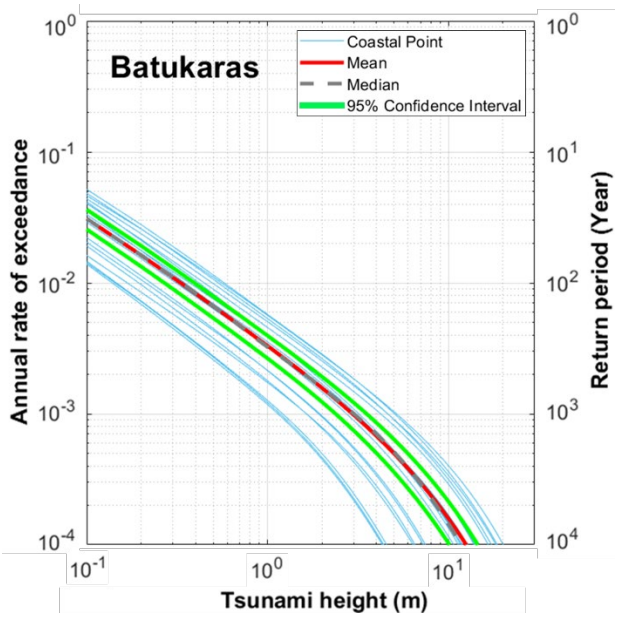

Figure 6 Tsunami hazard curves at each observation point (light blue) including mean and median value curves in Batukaras Village

The morphological conditions (shape) of the coast in Batukaras Village can be categorized into two types, namely steep and sloping coastal areas. When viewed from the distribution of observation points (coastal points) scattered along the coastline of Batukaras Village, the division of the two coastal morphologies can be seen in Figure 7.

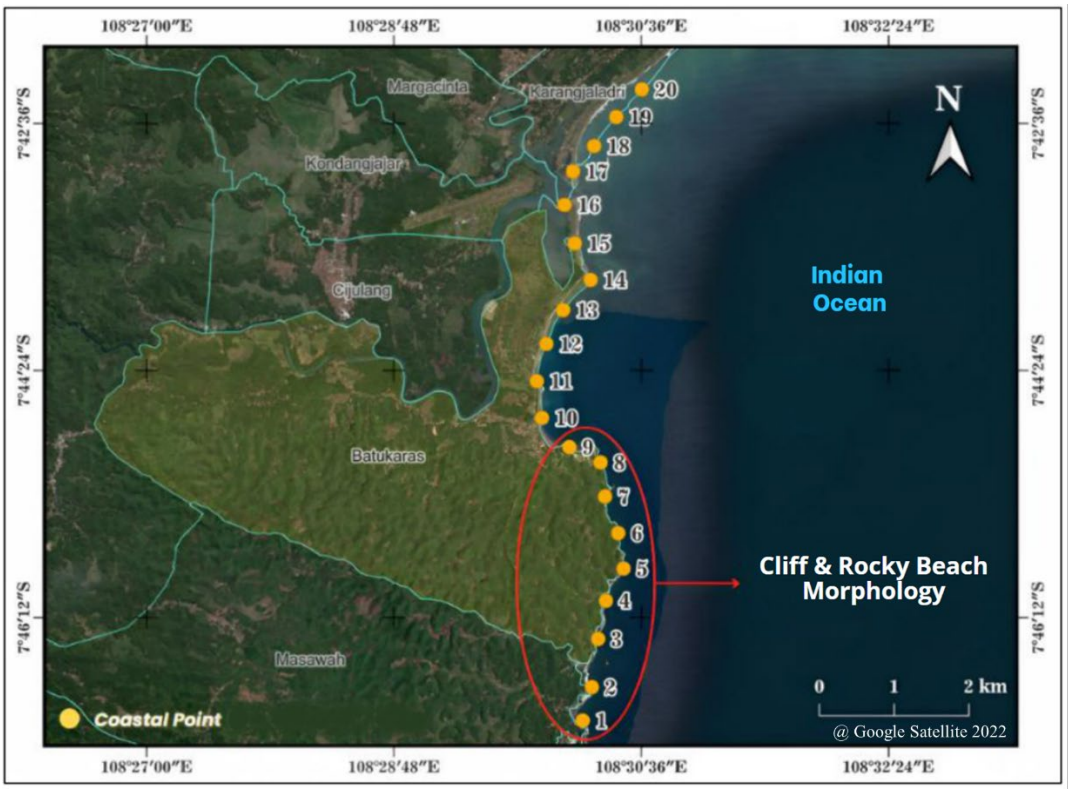

Figure 7 Beach morphology in Batukaras Village

Based on Figure 7, it can be seen that the 1st to 9th observation points are in the coastal area with steep morphology with characteristics of cliff and rocky beach. In contrast, the 10th to 20th observation points are located on the sloping coastal area in Batukaras Village. Therefore, in this PTHA in Batukaras Village, the tsunami height generated from the modeling results of the two types of coastal morphology is identified, which can be seen in Figure 8.

In the resulting hazard curve, a significant difference in average tsunami height can be seen between the two different coastal morphologies in Batukaras Village. In the coastal areas with steep morphology for an earthquake return period of 1000 years, the resulting average tsunami height is still below 10 meters (lower than the average tsunami height in Batukaras Village presented in Figure 6). In contrast, in coastal areas with a gentle sloping morphology, the average tsunami height is already above 10 meters (higher than the average tsunami height in Batukaras Village presented in Figure 6). This shows that the morphology of the coast in Batukaras Village will affect the height of the tsunami generated.

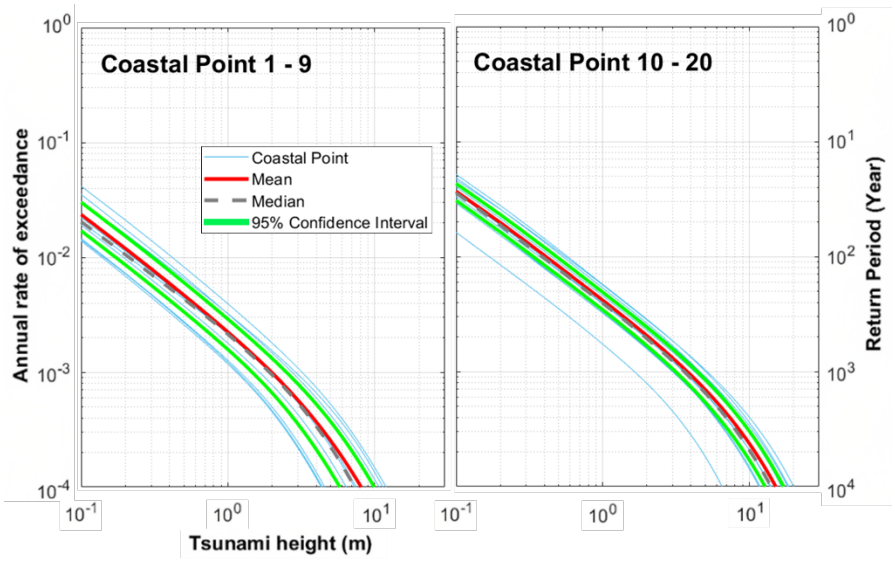

Figure 8 Tsunami hazard curves based on earthquake return period (a) Observation points 1 to 9; (b) Observation points 10 to 20.

3.2 Tsunami Heights Based on Earthquake Return Period

The second product of the PTHA can also be viewed in graphical form to identify the tsunami height at each observation point. In this case, the tsunami height in Batukaras Village was identified based on four types of earthquake return periods, namely 250 years, 500 years, 1000 years, and 2500 years. This graph can be seen in Figure 9.

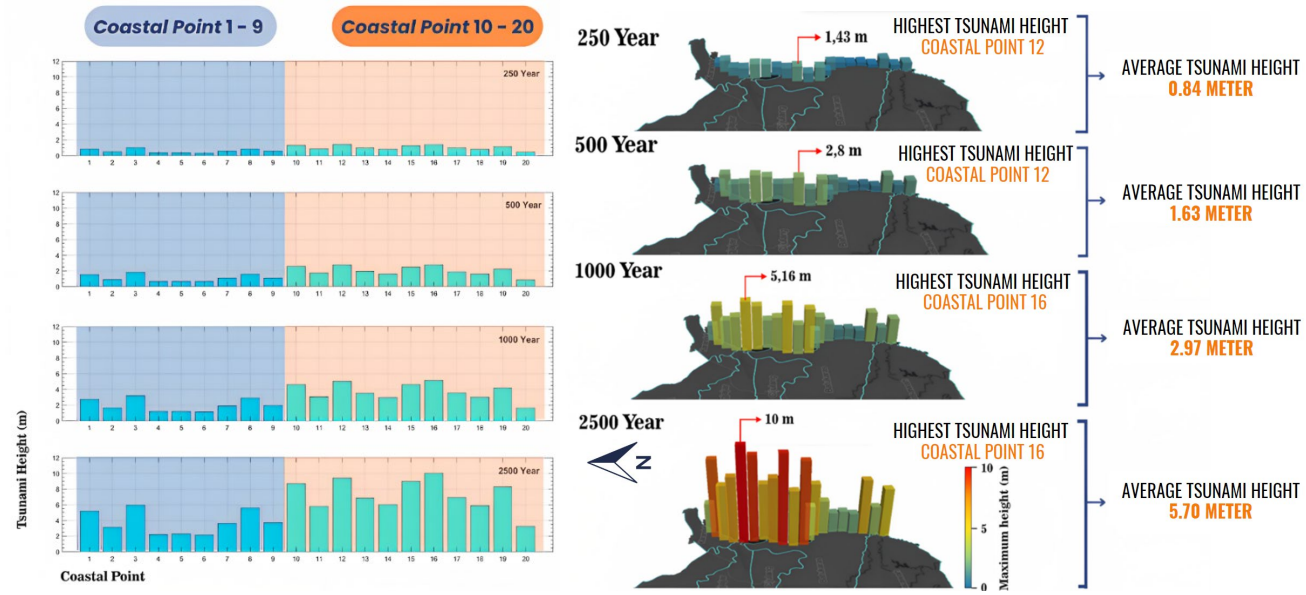

Figure 9 Visualization of tsunami height based on earthquake return period at each observation point

Figure 9 shows a graph of the tsunami height at each earthquake return period derived from the tsunami hazard curve in Figure 6. In this graph, the difference in tsunami height between the steep beach (1st to 9th observation points in the south area) and sloping beach (10th to 20th observation points in the north area) in Batukaras Village is clearly visible. Overall, tsunami heights at all observation points located on steep coastal areas were much lower than those on sloping coastal areas for each earthquake return period.

The average tsunami heights for sloping coastal areas are 0.58 m, 1.1 m, 1.98 m, and 3.75 m for each earthquake return period of 250 years, 500 years, 1000 years, and 2500 years, respectively. In contrast, the mean tsunami heights for steep coastal areas are 1.04 m, 2.05 m, 3.77 m, and 7.29 m for each of the 250-year, 500-year, 1000-year, and 2500-year return periods, respectively. Based on these values, it can be seen that there is a twofold difference in the average tsunami height between the sloping coastal areas and the steep coastal areas at each earthquake return period.

3.3 Results of Deaggregation of Hazard in Batukaras Village

Deaggregation of earthquake hazards will produce the most dominant average magnitude and distance that affect an area (Aprillianto, 2016). Based on the results of this PTHA, the hazard contribution of each megathrust segment that can have an influence on tsunami events in Batukaras Village can be known. This deaggregation value can be seen at each observation point used in this modelling.

Overall, if the hazard deaggregation values are averaged from all observation points scattered along the coastline of Batukaras Village, the tsunami hazard deaggregation in Batukaras Village can be obtained. The hazard deaggregation values of each of these megathrust segments for tsunami events can be seen in Figure 10.

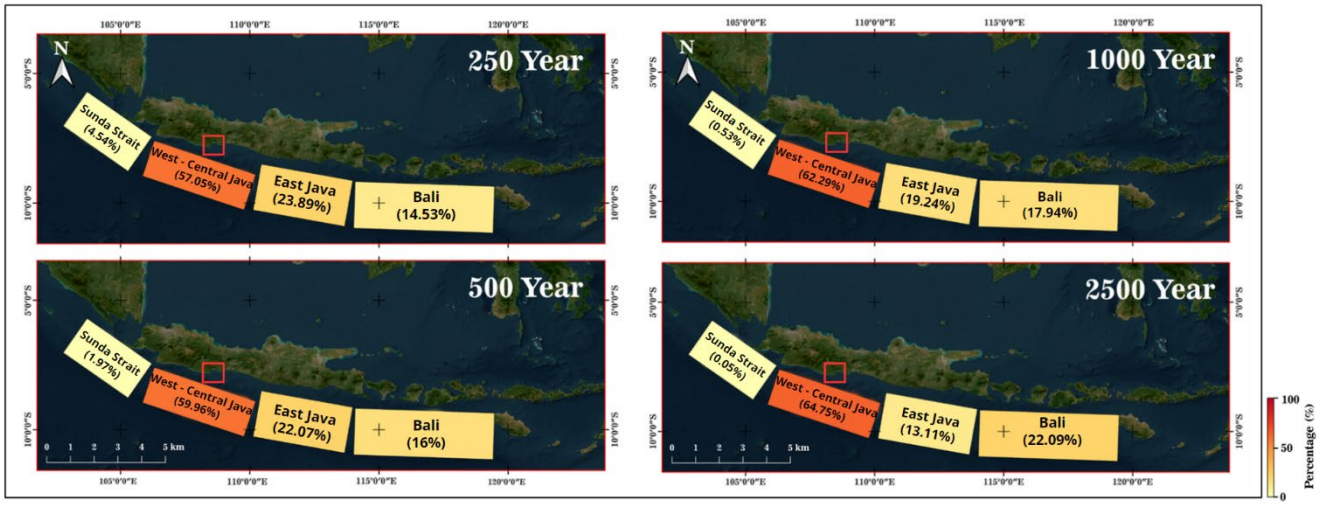

Figure 10 Deaggregation map of each megathrust segment based on earthquake return period

Based on the map, it can be seen the deaggregation of each megathrust segment based on the return period of an earthquake. In each earthquake return period, the deaggregation numbers for each megathrust segment can be seen in Table 3.

Table 3 Deaggregation of each megathrust segment based on earthquake return period

Segments	250 Year	500 Year	1000 Year	2500 Year	Description
Sunda Strait	4,54%	1,97%	0,53%	0,05%	**Decrease**
West – Central Java	57,05%	59,96%	62,29%	64,75%	**Increase**
East Java	23,89%	22,07%	19,24%	13,11%	**Decrease**
Bali	14,53%	16%	17,94%	22,09%	**Increase**

The table shows that the Sunda Strait megathrust segment has the smallest deaggregation for each earthquake return period. This is because the geographical location of this segment is in the western part of Batukaras Village. Thus, tsunami waves generated by an earthquake on this segment would be difficult to travel to Batukaras Village since it does not directly facing the Sunda Straits megathrust. In contrast, the deaggregation of the West Java-Central Java megathrust segment increases with each advancement of the earthquake return period. Geographically, this is because this segment is closest to and directly faces Batukaras Village. Therefore, if an earthquake occurs with an epicentre originating from this segment, the potential for the tsunami to reach Batukaras Village is quite high.

3.4 Results of Annual Probability of Tsunami Occurrence at Earthquake Return Periods

The final PTHA product is the annual probability value of a tsunami occurring in Batukaras Village for each observation point. Based on this, the PTHA results show the annual tsunami probability values for each observation point for tsunami heights greater than 0.5 m, 1.5 m, and 3 m. These probability values can be seen in Figure 10.

Based on the map, it can be seen that the probability of a tsunami in Batukaras Village is less than 0.1% in any given year. This probability value indicates a very small number of tsunami events in Batukaras Village. Such a result aligns with historical data, in which tsunami disasters are rare in Pangandaran Regency and its surroundings.

The probability for tsunami heights greater than 0.5 m in a given year, with a probability value greater than 0.04%, is only found at observation points located in sloping coastal areas. The probabilities for tsunami heights of more than 1.5 m and 3 m in a given year are less than 0.02% and 0.001% for all observation points, respectively. However, these probability values should not be used as the main reference because, like earthquakes, tsunamis can occur at any time.

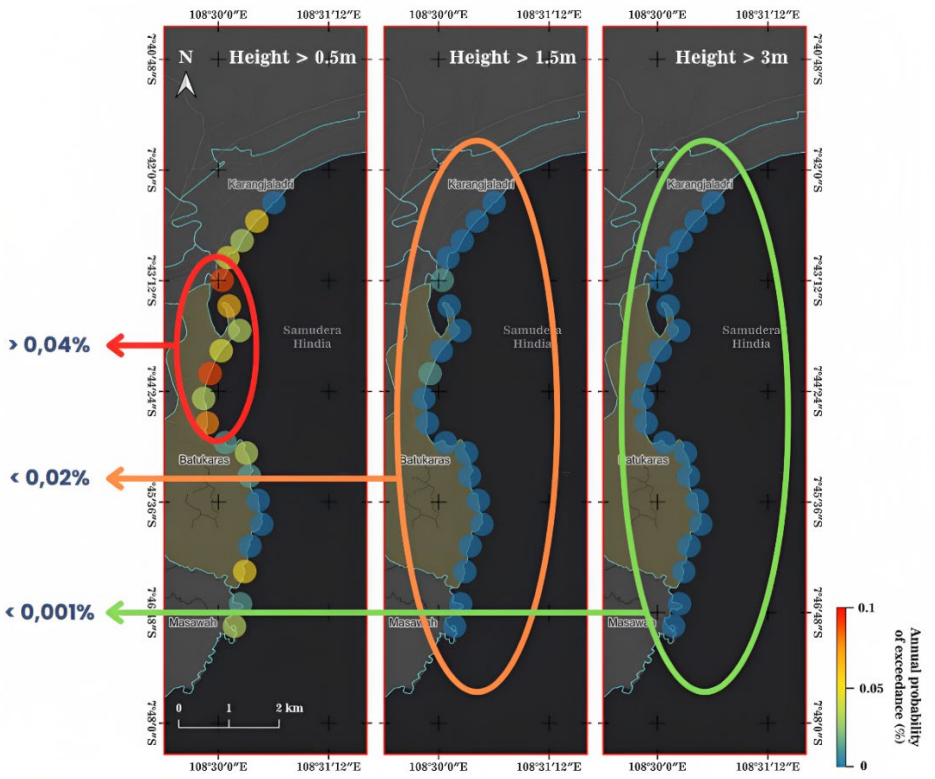

Figure 11 Annual probability of tsunami occurrence in Batukaras Village based on tsunami height (a) > 0.5m; (b) > 1.5m; (c) > 3m

4 Conclusion

The PTHA in Batukaras Village resulted in tsunami heights of 0.84 m, 1.63 m, 2.97 m, and 5.7 m for each earthquake return period of 250 years, 500 years, 1000 years, and 2500 years, respectively. The results of the tsunami hazard deaggregation in Batukaras Village show that the largest contribution of earthquake sources that can generate tsunamis in Batukaras Village comes from the West Java-Central Java megathrust segment, with a contribution value of more than 57% for each earthquake return period. This can serve as a tsunami warning for Batukaras Village in the event of a high-magnitude earthquake centred on the West Java-Central Java segment. Meanwhile, the annual probability value of tsunami occurrence in Batukaras Village with a height of 0.5 m, 1.5 m, and 3 m has a probability smaller than 0.1% in any given year.

Then, the results of the PTHA can be analysed in more detail by reviewing the tsunami height at each observation point. In the results of the hazard curve, different coastal morphologies produce different tsunami heights. The maximum tsunami height occurs in coastal areas with sloping morphology. This sloping coastal area is very vulnerable because it is dominated by lodging places and restaurants, making it vulnerable to tsunami disasters. Apart from the sloping coastal factor, the vulnerability of the Batukaras coast to tsunamis is also influenced by the social aspect, where the population in this village is

quite dense, reaching 393 inhabitants/km^2. Apart from being crowded with residents, the Batukaras coast is also a famous tourist attraction for foreign tourists. This contributes to the vulnerability of the Batukaras coast to tsunami disasters. The coastal area is also vulnerable from an economic perspective, because this coast is dominated by lodging, restaurants, and also agricultural land and plantations, which contribute to the village's regional income. The large amount of land that may be affected by the tsunami could cause significant economic losses for the surrounding community. The results of this PTHA modelling can be a reference in making disaster mitigation strategies and scenarios in Batukaras Village, especially for sloping beach areas. This is also considering that Batukaras Village is one of the tourist villages that is visited by many local and foreign tourists.

The results of this study can be used as a reference to conduct further research to calculate economic losses from buildings, land use, and other economic factors from tsunami disasters. In mitigation activities, the results of this research can be used to support the assessment components in preparing Batukaras village to become a tsunami ready village published by IOC-Unesco considering that Batukaras Village is currently in the recognition process.

References

Aida, I. (1978). Reliability of a tsunami source model derived from fault parameters. *Journal of Physics of the Earth*, 26(1), 57-73.

Annaka, T., Satake, K., Sakakiyama, T., Yanagisawa, K., Shuto, N. (2007). Logic-tree approach for probabilistic tsunami hazard analysis and its applications to the Japanese coasts. *Tsunami and its hazards in the Indian and Pacific Oceans*, 164, 577–592.

Batukaras Village Profile. (2022). *Batukaras Village Profile*. Pemerintah Kabupaten Pangandaran.

Cornell C. Allin. (1968). Engineering Seismic Risk Analysis. *Bulletin of the Seismological Society of America*, *58*(5), 1583–1606.

Davies, G., Grifn, J., Løvholt, F., Glimsdal, S., Harbitz, C., Thio, H. K., Lorito, S., Basili, R., Selva, J., Geist, E., Baptista, M. A. (2018). A global probabilistic tsunami hazard assessment from earthquake sources. *Geological Society London Special Publications*, 456(1), 219–244.

Fritz, H. M., Kongko, W., Moore, A., McAdoo, B., Goff, J., Harbitz, C., Uslu, B., Kalligeris, N., Suteja, D., Kalsum, K., Titov, V., Gusman, A., Latief, H., Santoso, E., Sujoko, S., Djulkarnaen, D., Sunendar, H., & Synolakis, C. (2007). Extreme runup from the 17 July 2006 Java tsunami. *Geophysical Research Letters*, *34*(12), 1–5. https://doi.org/10.1029/2007GL029404

Fujii, Y., & Satake, K. (2006). Source of the July 2006 West Java tsunami estimated from tide gauge records. *Geophysical Research Letters*, *33*(24), 1–5. https://doi.org/10.1029/2006GL028049

Fukutani, Y., Suppasri, A., & Imamura, F. (2015). Stochastic analysis and uncertainty assessment of tsunami wave height

using a random source parameter model that targets a Tohoku-type earthquake fault. *Stochastic Environmental Research and Risk Assessment*, 29, 1763-1779.

Grezio, A., Babeyko, A., Baptista, M. A., Behrens, J., Costa, A., Davies, G., Geist, E. L., Glimsdal, S., González, F. I., Griffin, J., Harbitz, C. B., LeVeque, R. J., Lorito, S., Løvholt, F., Omira, R., Mueller, C., Paris, R., Parsons, T., Polet, J., … Thio, H. K. (2017). Probabilistic Tsunami Hazard Analysis: Multiple Sources and Global Applications. *Reviews of Geophysics*, *55*(4), 1158–1198. https://doi.org/10.1002/2017RG000579

Gunawan, E., Meilano, I., Abidin, H. Z., Hanifa, N. R., & Susilo. (2016). Investigation of the best coseismic fault model of the 2006 Java tsunami earthquake based on mechanisms of postseismic deformation. *Journal of Asian Earth Sciences*, *117*, 64–72. https://doi.org/10.1016/j.jseaes.2015.12.003

Hamzah, L., Puspito, N. T., & Imamura, F. (2000). Tsunami Catalog and Zones in Indonesia. *Journal of Natural Disaster Science*, *22*(1), 25–43. https://doi.org/10.2328/jnds.22.25

Hanifa, N. R., Sagiya, T., Kimata, F., Efendi, J., Abidin, H. Z., & Meilano, I. (2014). Interplate coupling model off the southwestern coast of Java, Indonesia, based on continuous GPS data in 2008-2010. *Earth and Planetary Science Letters*, *401*, 159–171. https://doi.org/10.1016/j.epsl.2014.06.010

Harris, R., Meservy, W., Stuart, K., Deng, M., Emmett, C., & Suliaman, H. (2019). *Seismic and Tsunami Risk of the Java Trench and Implementation of Risk Reduction Strategies Seismic and Tsunami Hazards in Eastern Indonesia Downloaded 12 / 28 / 22 to 114 . 122 . 105 . 32 . Redistribution subject to SEG license or copyright ; see Terms o*. 4786–4789.

Hayes, G. P., Moore, G. L., Portner, D. E., Hearne, M., Flamme, H., Furtney, M., & Smoczyk, G. M. (2018). Slab2, a comprehensive subduction zone geometry model. *Science*, *362*(6410), 58–61. https://doi.org/10.1126/science.aat4723

Horspool, N., Pranantyo, I., Griffin, J., Latief, H., Natawidjaja, D. H., Kongko, W., Cipta, A., Bustaman, B., Anugrah, S. D., & Thio, H. K. (2014). A probabilistic tsunami hazard assessment for Indonesia. *Natural Hazards and Earth System Sciences*, *14*(11), 3105–3122. https://doi.org/10.5194/nhess-14-3105-2014

Koswara, D. V., Windupranata, W., Meilano, I., Hayatiningsih, I., & Hanifa, N. R. (2021). Characteristics of Potential Tsunami Evacuee and Evacuation Infrastucture in Pangandaran Beach, Indonesia. *IOP Conference Series: Earth and Environmental Science*, *925*(1). https://doi.org/10.1088/1755-1315/925/1/012036

Mulia, I. E., Gusman, A. R., Williamson, A. L., & Satake, K. (2019). An Optimized Array Configuration of Tsunami Observation Network Off Southern Java, Indonesia. *Journal of Geophysical Research: Solid Earth*, *124*(9), 9622–9637. https://doi.org/10.1029/2019JB017600

Mustafida, R. P., Veronica, N., Karima, A. Q., De Silva Nusantara, C. A., & Windupranata, W. (2022). Identification of the IOC-UNESCO Tsunami Ready Indicator to Improve Coastal Community Preparedness for Tsunami Disaster in Batukaras Village, Pangandaran Regency, Indonesia. *2022 IEEE Asia-Pacific Conference on Geoscience, Electronics and Remote Sensing Technology: Understanding the Interaction of Land, Ocean, and Atmosphere: Smart City and Disaster Mitigation for Regional Resilience, AGERS 2022 - Proceeding*, 41–47.

https://doi.org/10.1109/AGERS56232.2022.10093500

Nijman, V. (2021). Tourism Developments Increase Tsunami Disaster Risk in Pangandaran, West Java, Indonesia. *International Journal of Disaster Risk Science*, *12*(5), 764–769. https://doi.org/10.1007/s13753-021-00365-3

Salmanidou, D. M., Heidarzadeh, M., & Guillas, S. (2019). Probabilistic Landslide-Generated Tsunamis in the Indus Canyon, NW Indian Ocean, Using Statistical Emulation. *Pure and Applied Geophysics*, *176*(7), 3099–3114. https://doi.org/10.1007/s00024-019-02187-3

Supendi, P., Widiyantoro, S., Rawlinson, N., Yatimantoro, T., Muhari, A., Hanifa, N. R., Gunawan, E., Shiddiqi, H. A., Imran, I., Anugrah, S. D., Daryono, D., Prayitno, B. S., Adi, S. P., Karnawati, D., Faizal, L., & Damanik, R. (2023). On the potential for megathrust earthquakes and tsunamis off the southern coast of West Java and southeast Sumatra, Indonesia. *Natural Hazards*, *116*(1), 1315–1328. https://doi.org/10.1007/s11069-022-05696-y

Windupranata, W., Hanifa, N. R., Nusantara, C. A. D. S., Aristawati, G., & Arifianto, M. R. (2020). Analysis of tsunami hazard in the Southern Coast of West Java Province - Indonesia. *IOP Conference Series: Earth and Environmental Science*, *618*(1). https://doi.org/10.1088/1755-1315/618/1/012026

World Health Organization. (2023). Weekly epidemiological update on COVID-19 – 11 May 2023. Accessed on 16 May 2023, dari https://www.who.int/publications/m/item/weekly-epidemiological-update-on-covid-19---11-may-2023